

Adapted variable density subsampling for compressed sensing

Simon Ruetz

*University of Innsbruck
Technikerstraße 13
6020 Innsbruck, Austria*

SIMON.RUETZ@UIBK.AC.AT

Abstract

Recent results in compressed sensing showed that the optimal subsampling strategy should take into account the sparsity pattern of the signal at hand. This oracle-like knowledge, even though desirable, nevertheless remains elusive in most practical application. We try to close this gap by showing how the sparsity patterns can instead be characterised via a probability distribution on the supports of the sparse signals allowing us to again derive optimal subsampling strategies. This probability distribution can be easily estimated from signals of the same signal class, achieving state of the art performance in numerical experiments. Our approach also extends to structured acquisition, where instead of isolated measurements, blocks of measurements are taken.

1. Compressed Sensing

Let $x \in \mathbb{C}^K$ be some signal and $A \in \mathbb{C}^{m \times K}$ be some matrix. Compressed sensing (CS) consists of reconstructing the signal x from measurements $y = Ax$. Usually it is assumed that the signal x is S -sparse, meaning that only $S \ll K$ elements of x are non-zero. Thus one tries to solve the following optimisation problem

$$\hat{x} = \arg \min \|x\|_1 \quad \text{s.t.} \quad y = Ax. \quad (1)$$

Starting with the seminal works [8, 13], compressed sensing theory tries to find sufficient conditions for the above minimisation problem to recover the the sparse signal. Early results suggested that if each entry of the matrix A is sampled i.i.d. from a Gaussian distribution and $m \gtrsim S \log(K)$, then the above minimisation does yield the correct solution with high probability.

These results were very soon extended to a random subsampling setting, where the sensing matrix A is constructed by sampling rows a_k from a unitary matrix $A_0 \in \mathbb{C}^{K \times K}$ uniformly at random [7, 22]. In this setting, a typical sufficient condition for the above minimisation problem to recover the sparse signal with probability at least $1 - \varepsilon$ reads as

$$m \gtrsim SK \max_{1 \leq k \leq K} \|a_k\|_\infty^2 \log(K/\varepsilon). \quad (2)$$

If A_0 is the discrete Fourier matrix — for which $\max_{1 \leq k \leq K} \|a_k\|_\infty^2 = \frac{1}{K}$ — this leads to theoretical results comparable to the Gaussian setting. Nevertheless this still falls short of explaining the remarkable success of CS in most applications where $K \max_{1 \leq k \leq K} \|a_k\|_\infty^2$ is

usually quite large.

To solve this problem, variable density subsampling was introduced [22, 10, 21, 9, 18]. There the sensing matrix $A \in \mathbb{C}^{m \times K}$ is constructed by sampling the rows of A_0 via a (possibly non-uniform) probability distribution. Concretely, the sensing matrix A is defined to be

$$A := \frac{1}{\sqrt{m}} \left(\frac{1}{\sqrt{\pi_{j_\ell}}} a_{j_\ell} \right)_{1 \leq \ell \leq m},$$

where m is the number of measurements we are allowed to take and j_ℓ for $1 \leq \ell \leq m$ are i.i.d random variables such that $\mathbb{P}(j_\ell = k) = \pi_k$. Note that the subsampling strategy is determined by the probabilities π_k for $1 \leq k \leq K$. A typical choice in this setting is $\pi_k := \frac{\|a_k\|_\infty^2}{\sum_k \|a_k\|_\infty^2}$ leading to the sufficient condition

$$m \gtrsim S \sum_k \|a_k\|_\infty^2 \log(K/\varepsilon).$$

This is nevertheless still not enough to completely bridge the gap between theory and application. Recent results go further by arguing that the optimal subsampling strategy should not only depend on the sensing and sparsity matrices, but also on the structure of the sparse signals [2, 5, 3]. The so called flip test proposed in [2] is a prime example of this fact. The assumption of knowledge of the structure of the sparse signals was also shown to be especially important in the case of blocks of measurements [5, 11, 3]. The drawback of all of these results is that they rely on the exact knowledge of the locations of the non-zero coefficients of the sparse signal, which may not be available in practice.

2. Contribution

In this paper we generalise these results to show how the subsampling strategy depends on the **distribution** of sparse supports together with the structure of the sensing/sparsity matrix. We are able to do this by assuming that the sparse supports follow a (possibly) non-uniform distribution, thereby generalising the aforementioned results. In practice, if one has access to a number of *similar* signals to x , a guess of the underlying distribution of sparse supports of x can be made and the optimal subsampling pattern be thus derived. We also extend our results to the setting of structured acquisition, where instead of isolated measurements, blocks of measurements are taken. In Section 3 we introduce the relevant notation, Section 4 states the main result, Section 5 applies our theory to some special cases to compare it to existing results and Section 6 shows how to apply this result in practice. The proof of our main result is stated in Section 7.

3. Notation and setting

A quick note on the notation used throughout this text. The vectors $(e_i)_{1 \leq i \leq K}$ denote the vectors of the canonical basis of \mathbb{R}^K . Let $A \in \mathbb{C}^{d \times K}$. We denote by A_k and A^k the k -th column and k -th row of A respectively and by A^* the conjugate transpose of the matrix A . For $1 \leq p, q, r \leq \infty$ we set $\|A\|_{p,q} := \max_{\|x\|_q=1} \|Ax\|_p$. Recall that $\|AB\|_{p,q} \leq \|A\|_{q,r} \|B\|_{r,p}$

and $\|Ax\|_q \leq \|A\|_{q,p} \|x\|_p$. A frequently encountered quantity is

$$\|A\|_{\infty,2} = \max_{k \in \{1, \dots, d\}} \|A^k\|_2,$$

which denotes the maximum ℓ_2 row norm of A . For ease of notation we sometimes write $\|A\| = \|A\|_{2,2}$ for the largest absolute singular value of A . For a vector $v \in \mathbb{R}^d$, we denote $\|v\|_{\max} := \|v\|_{\infty}$ the maximal entry of v . For a subset $I \subseteq \mathbb{K} := \{1, \dots, K\}$, called the support, we denote by A_I the submatrix with columns indexed by I . Further for a support I , we set $R_I := \mathbb{I}_I \in \mathbb{R}^{K \times |I|}$, allowing us to write $A_I = AR_I$. We denote by $A_{k,:}$ (resp. $A_{:,k}$) the k -th row (resp. column) of A and by $A_{J,L}$ the submatrix with rows indexed by J and columns indexed by L . We denote by $\text{vec} : \mathbb{C}^{\sqrt{K} \times \sqrt{K}} \mapsto \mathbb{C}^K$ the vectorisation operation that transforms a complex matrix into a complex vector by stacking the columns on top of each other and by vec^{-1} its inverse. As was noted in the introduction we want the supports of our signals to follow a non-uniform distribution. We are going to use the following probability measure on $\mathcal{P}(\mathbb{K})$ that allow us to model non-uniform distributions for our supports.

Definition 1 (Rejective sampling - Conditional Bernoulli model) *Let $0 \leq \omega_j \leq 1$ be such that $\sum_{j=1}^K \omega_j = S$. We say our supports follow the rejective sampling model, if each support $I \subseteq \mathbb{K}$ is chosen with probability*

$$\mathbb{P}(I) := \begin{cases} c \prod_{i \in I} \omega_i \prod_{j \notin I} (1 - \omega_j) & \text{if } |I| = S \\ 0 & \text{else} \end{cases}, \quad (3)$$

where c is a constant to ensure that \mathbb{P} is a probability measure. We define the $D_{\omega} := \text{diag}((\omega_k)_k)$ as the square diagonal matrix with the weight vector ω on its diagonal. We call $W \in \mathbb{R}^{\sqrt{K} \times \sqrt{K}}$ the weight matrix, if $\text{vec}(W) = \omega$.

This lets us define the following model for our signals.

Definition 2 (Signal model) *We model our signals as*

$$x = \sum_{i \in I} e_i x_i, \quad \text{sign}(x_i) = \sigma_i, \quad \forall i \in I, \quad (4)$$

where $I = \{i_1, \dots, i_S\}$ is the random support following either the rejective or Poisson sampling model with weight vector ω such that $\sum_{i=1}^K \omega_i = S$ and denote by D_{ω} the corresponding diagonal matrix. Further we assume that the signs σ_i form a Rademacher sequence, i.e. $\sigma_i = \pm 1$ with equal probability.

4. Main result

Our notation will follow the notation in [5] very closely with the main difference being the randomness of the sparse support (see above) and the sampling model of the measurements. Assume we are given an unitary matrix $A_0 \in \mathbb{C}^{K \times K}$ representing the set of possible linear measurements $(A_0^*)_i =: a_i^*$. We partition the set $\{1, \dots, K\}$ into M blocks \mathcal{I}_k such that $\uplus_k \mathcal{I}_k = \{1, \dots, K\}$ and set

$$B_k := (a_i)_{i \in \mathcal{I}_k} \in \mathbb{C}^{|\mathcal{I}_k| \times K}$$

The sensing matrix A is then defined as

$$A := \frac{1}{\sqrt{m}} \left(\frac{1}{\sqrt{\pi_{j_\ell}}} B_{j_\ell} \right)_{1 \leq \ell \leq m},$$

where $m \leq M$ is the number of blocks we want to measure and j_ℓ for $1 \leq \ell \leq m$ are i.i.d random variables such that $\mathbb{P}(j_\ell = k) = \pi_k$. So the π_k define the probability with which each block of measurements gets selected. We call

$$\max_k \|a_k\|_\infty^2, \quad (5)$$

the coherence of the matrix A_0 . With these definitions we are finally able to state our main result.

Theorem 3 *Assume that the signals follow the model in 2, where the support $I \subseteq \mathbb{K}$ is chosen according to the rejective sampling model with probabilities $\omega_1, \dots, \omega_K$ such that $\sum_{k=1}^K \omega_k = S$ and $0 < \omega_k \leq 1$. If the measurements B_k are sampled according to probabilities π_k and if*

$$\begin{aligned} m &\gtrsim \max_k \frac{\|B_k^* B_k\|_{\infty,1}}{\pi_k} \log^3(K/\varepsilon), \\ m &\gtrsim \max_k \frac{\|B_k D_\omega B_k^*\|_{2,2}}{\pi_k} \log^2(K/\varepsilon), \end{aligned} \quad (6)$$

then (1) recovers the sparse signal with probability $1 - \varepsilon$.

The exact statement — including constants — can be found in Section 7. The restriction $\omega > 0$ is no hard constraint, as in the case of $\omega_i = 0$ for some i , a careful analysis of the proof shows that one can then set the columns of A_{J^c} to zero, as they will never get used by the random supports I .

The above result shows that the optimal sampling strategy π should depend both on the distribution of sparse supports ω via the diagonal matrix D_ω and on the structure of the blocks B_k . One way to optimise the above bounds is by setting

$$\pi_k := \frac{\max \{\|B_k D_\omega B_k^*\|_{2,2}, \|B_k^* B_k\|_{\infty,1}\}}{L}, \quad (7)$$

where L is a normalising constant ensuring $\sum_k \pi_k = 1$. By plugging this bound into the above Theorem we get that we need about

$$m \gtrsim \left(\sum_k \|B_k D_\omega B_k^*\|_{2,2} + \sum_k \|B_k^* B_k\|_{\infty,1} \right) \log^3(K/\varepsilon) \quad (8)$$

measurements to ensure recovery with high probability. In Section 5 we will look at special cases of blocks of measurements, where this bound on m can be further simplified. For isolated measurements, i.e. $B_k = a_k$ the above can be further simplified to yield the following result.

Corollary 4 Assume that the signals follow the model in 2, where the support $I \subseteq \mathbb{K}$ is chosen according to the rejective sampling model with probabilities $\omega_1, \dots, \omega_K$ such that $\sum_{k=1}^K \omega_k = S$ and $0 < \omega_k \leq 1$. If the measurements a_k are sampled according to

$$\pi_k = \frac{\max\{a_k D_\omega a_k^*, \|a_k\|_\infty^2\}}{L}, \quad (9)$$

where L is a normalising constant ensuring $\sum_k \pi_k = 1$, and if

$$m \gtrsim \left(S + \sum_k \|a_k\|_\infty^2 \right) \log^3(K/\varepsilon), \quad (10)$$

then (1) recovers the sparse signal with probability $1 - \varepsilon$.

Proof First note that $\|B_k D_\omega B_k^*\|_{2,2} = a_k D_\omega a_k^*$ and thus

$$\sum_k a_k D_\omega a_k^* = \text{tr}(A_0 D_\omega A_0^*) = \text{tr}(D_\omega) = S.$$

Further

$$\|B_k^* B_k\|_{\infty,1} = \|a_k^* a_k\|_{\infty,1} \leq \max_{i,j} |a_{k,i} a_{k,j}| \leq \max_i |a_{k,i}|^2 = \|a_k\|_\infty^2,$$

leading to $L \leq S + \sum_k \|a_k\|_\infty^2$. Plugging these π_k into Theorem 3 yields the result. \blacksquare

This result is an improvement upon standard results for general (unknown) supports I , which read $m \gtrsim S \sum_k \|a_k\|_\infty^2 \log(K)$ [7, 21, 18, 9]. This is to be expected since we assume more information about the supports and their distribution. On the other hand, the additional log factors are the price we pay for our random signal approach. A comparison to existing results that assume knowledge about the structure of sparsity, which will be done in the next section, will thus be more interesting.

Further, Corollary 4 shows how, for a given weight vector ω , this lower bound is attained via formula (9). This is an easy-to-use recipe yielding state of the art results in a number of experiments (see Sections 5 and 6). Before moving on to empirical results, we want to mention a few special cases of measurement matrices Φ , sparsity basis Ψ and weights ω which underline the generality of the above result.

5. Special cases

In this section we show how our result can be applied to recover state of the art theoretical results in CS theory.

5.1 Sparsity in levels

A frequent assumption in modern compressed sensing theory is sparsity in levels [2, 5, 3]. To apply our results to this framework we assume that $K = 2^{J+1}$ for some $J \in \mathbb{N}$ and set $A_0 = \mathcal{F}\Psi^*$, where \mathcal{F} is the 1-D Fourier transform with rows indexed from $-K/2 + 1$ to $K/2$ and Ψ is the 1-D inverse Haar wavelet transform. Denote by Ω the dyadic partition of the set $\{1, \dots, K\}$ where $\Omega_0 := 0$ and $\Omega_j := \{2^j + 1, \dots, 2^{j+1}\}$ for $j = 1, \dots, J$. Further

denote by Ω the r frequency bands of the discrete Fourier transform \mathcal{F} , i.e., $M_0 := \{0, 1\}$ and $M_j := \{-2^j + 1, \dots, -2^{j-1}\} \cup \{2^{j-1} + 1, \dots, 2^j\}$ for $j = 1, \dots, J$, then Lemma 1 in [1] states that for $\ell \in W_i$ and $k \in \Omega_j$

$$|a_{k,\ell}|^2 \lesssim 2^{-j} 2^{|j-i|}. \quad (11)$$

We define the **average sparsity in levels**

$$S_\ell := \|\omega_{\Omega_\ell}\|_1 \quad (12)$$

For simplicity we assume $S_\ell > 1$ for all $1 \leq \ell \leq J$. Plugging this into (9) yields for $k \in M_j$

$$\|a_k D_\omega^{1/2}\|_2^2 \lesssim 2^{-j} S_j + 2^{-j} \sum_{p \neq j} 2^{|j-p|} S_p, \quad (13)$$

and thus by using π as defined in (9) our main result yields the sufficient condition

$$m \gtrsim \left(\sum_{\ell} S_\ell + \sum_{p \neq j} 2^{|j-p|} S_p \right) \log^3(K/\varepsilon), \quad (14)$$

in line with results in [3].

5.2 Blocks of measurements

Even though the above sampling strategies yield very good reconstruction results, probing measurements independently at random is infeasible — or at least impractical — in most real applications, see [5] and references therein. Luckily, our results easily extend to the case of blocks of measurements B_k .

5.2.1 SENSING VERTICAL (OR HORIZONTAL) LINES IN 2D

We will again follow the notation in [5, 3] very closely to facilitate easier comparison. Assume again that $K = 2^{J+1}$ for some $J \in \mathbb{N}$. Let $\phi \in \mathbb{C}^{\sqrt{K} \times \sqrt{K}}$ be a unitary matrix (for example the 1D Fourier-Haar transform) and assume that our set of possible measurements is given by

$$A_0 = \phi \otimes \phi \in \mathbb{C}^{K \times K}. \quad (15)$$

With this notation, we define blocks of measurements which, in a 2D Fourier-Wavelet setting would correspond to vertical lines in frequency space. For this set

$$B_k := \phi_{k,:} \otimes \phi = \left(\phi_{k,1} \phi \mid \dots \mid \phi_{k,\sqrt{K}} \phi \right) \in \mathbb{C}^{\sqrt{K} \times K} \quad \text{for all } 1 \leq k \leq \sqrt{K}. \quad (16)$$

This setting allows us to model a more realistic setting and has the big advantage that the matrix $B_k^* B_k$ has a very nice representation. Note that in our main result we have to control $\|B_k D_\omega B_k^*\| = \|D_\omega^{1/2} B_k^* B_k D_\omega^{1/2}\|$. Using that ϕ is a unitary matrix we see

$$B_k^* B_k = (\phi_{k,:} \otimes \phi)^* (\phi_{k,:} \otimes \phi) = (\phi_{k,:}^* \phi_{k,:} \otimes \phi^* \phi) = (\phi_{k,:}^* \phi_{k,:} \otimes \mathbb{I}), \quad (17)$$

where \otimes denotes the Kronecker product. For our weight vector $\omega \in \mathbb{R}^K$ we denote by $W \in \mathbb{R}^{\sqrt{K} \times \sqrt{K}}$ the matrix such that $\text{vec}(W) = \omega$. Multiplying $B_k^* B_k = (\phi_{k,:}^* \phi_{k,:} \otimes \mathbb{I})$ from left and right with the diagonal matrix $D_\omega^{1/2}$ and taking the operator norm yields

$$\|D_\omega^{1/2}(\phi_{k,:}^* \phi_{k,:} \otimes \mathbb{I})D_\omega^{1/2}\| = \|D_\omega^{1/2} \begin{pmatrix} \phi_{k,1}^* \phi_{k,1} \mathbb{I} & \dots & \phi_{k,1}^* \phi_{k,\sqrt{K}} \mathbb{I} \\ \vdots & \ddots & \vdots \\ \phi_{k,\sqrt{K}}^* \phi_{k,1} \mathbb{I} & \dots & \phi_{k,\sqrt{K}}^* \phi_{k,\sqrt{K}} \mathbb{I} \end{pmatrix} D_\omega^{1/2}\|. \quad (18)$$

Since reordering of columns and rows does not change the operator norm, we apply the reordering $R : J = (1, \dots, K) \mapsto \text{vec}(\text{vec}^{-1}(J)^*)$ to both the columns and rows of the above matrix and set $\omega' := R(\omega)$ to get

$$\|D_\omega^{1/2}(\phi_{k,:}^* \phi_{k,:} \otimes \mathbb{I})D_\omega^{1/2}\| = \|D_{\omega'}^{1/2} \begin{pmatrix} \phi_{k,:}^* \phi_{k,:} & \dots & 0 \\ \vdots & \ddots & \vdots \\ 0 & \dots & \phi_{k,:}^* \phi_{k,:} \end{pmatrix} D_{\omega'}^{1/2}\| \quad (19)$$

$$= \max_{1 \leq \ell \leq \sqrt{K}} \|\phi_{k,:} D_{W_{\ell,:}}^{1/2}\|_2^2 = \max_{1 \leq \ell \leq \sqrt{K}} \sum_{i=1}^{\sqrt{K}} |\phi_{k,i}|^2 W_{\ell,i}. \quad (20)$$

So we look for the row v of the weight matrix W , such that $\|\phi_{k,:} D_v^{1/2}\|_2^2$ gets maximised. This encapsulates the relationship between the structure of the blocks of measurements and the structure of the sparse signals via its distribution. By the same argument as above we also see that

$$\|B_k^* B_k\|_{\infty,1} = \|\phi_k\|_\infty^2. \quad (21)$$

Plugging this into our formula for blocks (7) yields

$$\pi_k := \max \left\{ \max_{1 \leq \ell \leq \sqrt{K}} \sum_{i=1}^{\sqrt{K}} |\phi_{k,i}|^2 W_{\ell,i}, \|\pi_k\|_\infty^2 \right\} / L, \quad (22)$$

where L is the normalisation factor. If instead of vertical lines one would take horizontal lines, i.e.,

$$B_k := \phi \otimes \phi_{k,:} \quad (23)$$

we have

$$B_k^* B_k = \begin{pmatrix} \phi_{k,:}^* \phi_{k,:} & \dots & 0 \\ \vdots & \ddots & \vdots \\ 0 & \dots & \phi_{k,:}^* \phi_{k,:} \end{pmatrix} \quad (24)$$

without any reordering. Hence in this case

$$\|D_\omega^{1/2} B_k^* B_k D_\omega^{1/2}\| = \max_{1 \leq \ell \leq \sqrt{K}} \sum_{i=1}^{\sqrt{K}} |\phi_{k,i}|^2 W_{i,\ell}, \quad (25)$$

so we take the maximum over all columns of the weight matrix W . Plugging this into our formula for blocks (7) yields

$$\pi_k := \max \left\{ \max_{1 \leq \ell \leq \sqrt{K}} \sum_{i=1}^{\sqrt{K}} |\phi_{k,i}|^2 W_{i,\ell}, \|\pi_k\|_\infty^2 \right\} / L, \quad (26)$$

where L is the normalisation factor.

5.2.2 VERTICAL FOURIER-HAAR LINES

We now apply the above analysis to the special case where $\phi = \mathcal{FH}^*$ is the 1D Fourier-Haar transform. This yields that A_0 is the separable 2D Fourier-Haar transform¹. Define the weight matrix $W \in \mathbb{R}^{\sqrt{K} \times \sqrt{K}}$ such that $\text{vec}(W) = \omega$ for some weight vector ω . We again denote by M_ℓ the frequency bands of the one dimensional Fourier transform and by Ω_ℓ the dyadic partition (see previous subsection). In the 2D setting we define the **average sparsity in level ℓ** as

$$S_\ell^r := \max_k \|W_{k, \Omega_\ell}\|_1. \quad (27)$$

This is equivalent to the 1D case up to taking the maximum over all rows of the weight matrix W . Using (11) and assuming that $S_\ell^r > 1$ for all $1 \leq \ell \leq J$, the above analysis yields for $k \in M_j$

$$\|B_k^* D_\omega B_k\| = \max_{1 \leq \ell \leq \sqrt{K}} \sum_{i=1}^{\sqrt{K}} |\phi_{k,i}|^2 W_{\ell,i} \leq \sum_{i=1}^{\sqrt{K}} \max_{1 \leq \ell \leq \sqrt{K}} |\phi_{k,i}|^2 W_{\ell,i} \quad (28)$$

$$\lesssim 2^{-j} S_j^r + 2^{-j} \sum_{p \neq j} 2^{|j-p|} S_p^r, \quad (29)$$

and thus by using π as defined in (22) our main result yields the sufficient condition

$$m \gtrsim \left(\sum_{\ell} S_\ell^r + \sum_{p \neq j} 2^{|j-p|} S_p^r \right) \log^3(K/\varepsilon), \quad (30)$$

in line with results in [3]. Note that the first inequality in (29) is rather crude potentially loses a lot of information about the relationship between the weight matrix W and the structure of the matrix A_0 . This is why in our experiments we will stick with the quantity $\|B_k^* D_\omega B_k\| = \max_{1 \leq \ell \leq \sqrt{K}} \sum_{i=1}^{\sqrt{K}} |\phi_{k,i}|^2 W_{\ell,i}$.

5.3 Coherent matrix

Another frequent example showing the necessity of some sort of knowledge of the structure in sparse signals is the special case where $A_0 = \mathbb{I}$. Denote by $J := \{i : \omega_i \neq 0\}$ the set of indices, where the weights of our random support model are zero and set the columns

1. In all other experiments we use non-separable 2D wavelet transforms.

of A_{J^c} to zero. In this setting, formula (9) leads to $\pi_k = \frac{\delta_{k,J}}{|J|}$ and thus $m \gtrsim |J| \log^3(K/\varepsilon)$ which means that to ensure recovery with high probability, we have to sample all rows corresponding to positive weights ω_ℓ , i.e. all those rows that correspond to entries of our sparse vector that have a non-zero probability of appearing in the support. This also includes the setting where $\omega \in \{0, 1\}$ recovering, up to logarithmic factors, results derived in [5].

5.4 Fourier matrix

Assume that $A_0 = \mathcal{F}$, i.e. the 1-D Fourier transform. This matrix is known to be incoherent ($\|a_k\|_\infty^2 = \frac{1}{K}$) and in the isolated measurement setting this yields $a_k D_\omega a_k^* = \sum_\ell |a_{k,\ell}| \omega_\ell = \sum_\ell \frac{1}{K} \omega_\ell = \frac{S}{K}$ for any weight vector ω (recall that we have $\sum_\ell \omega_\ell = S$). Plugging these observations back into our main Theorem yields that independently of the distribution ω , one should sample uniformly at random, i.e. $\pi_k = \frac{1}{K}$. Corollary 4 thus yields $m \gtrsim S \log^3(K)$ which (excluding log factors) is in line with standard lower bounds on the number of measurements [8, 12].

5.5 Uniformly distributed sparse supports

One possible distribution of our sparse supports is the uniform distribution, where $\omega_\ell = S/K$. Plugging this into formula (9) yields

$$\pi_k = \frac{\max\{S/K, \|a_k\|_\infty^2\}}{L},$$

where L again is a normalising constant. This is very similar in spirit to the coherence based subsampling strategies, where $\pi_k := \frac{\|a_k\|_\infty^2}{\sum_\ell \|a_\ell\|_\infty^2}$ [22, 10, 21]. Since in the uniform case there is no structure in the sparse signals that can influence the subsampling strategy it is only natural that in this special case the optimal subsampling strategy depends more on the structure of the sensing matrix together with a lower bound S/K . We conduct a small experiment by setting $K = 2^{16}$ and $S = \sqrt{K}/2$. Further we let Φ be the 2D Hadamard transform and Ψ be the 2D Haar wavelet transform. We then generate 100 synthetic signals with uniformly distributed sparse supports and random signs to compare the performance of three different subsampling strategies, which can be seen in Figure 1. Sampling 5% of measurements from each of these distributions and subsequently solving 1 with the NESTA algorithm [20, 4] and averaging over 10 runs shows that our adapted subsampling strategy outperforms both the uniform and the coherence bases subsampling strategy. This shows that in this special case our result is tight in the sense that both terms in the numerator of formula 9 are indeed necessary.

6. Application

Now that we have seen that our theory is in line with recent results, we show where the true strengths of our result lies. We conduct a few experiments, in each of which we assume to be given a training set of images from which we generate the sparse distribution model by transforming them into a wavelet basis before applying a threshold. The relative frequency with which each coefficient appears in these sparse supports is our proxy for the inclusion

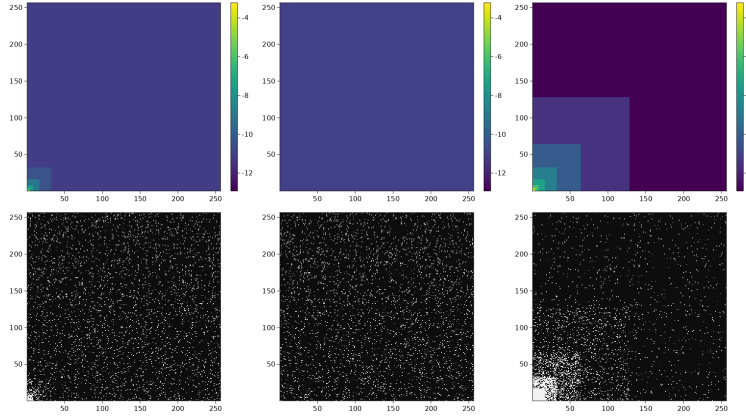


Figure 1: Subsampling densities (top row) and corresponding samples (bottom row) for the adapted variable density sampling scheme (left column), the uniform distribution (middle right) and the coherence based subsampling scheme (right row). The resulting average PSNR are: Adapted - 133.5, Uniform - 105.6 and Coherence - 62.3.

probabilities ω . This one-to-one correspondence motivated by the close relationship between the rejective sampling model and the Bernoulli sampling model with weights ω . We further assume to be given a reference image which we have to reconstruct. We will compare the performance of our subsampling strategy in the isolated measurement case against a state-of-the-art variable density subsampling scheme with polynomial decay, where we pick a frequency (k_1, k_2) in the 2D k-space with probability $\frac{1}{(k_1^2 + k_2^2)^{2.5}}$. To ensure meaningful results, each experiment is averaged over 10 runs. We will use the 2D Fourier matrix to take measurements and plot all sensing distributions in log-scale.

For our first experiment (Figure 2) we assume a standard compressed sensing setup with isolated 2D Fourier measurements and a 2D DB4 wavelet matrix as sparsifying matrix. We want to sense the reference brain image (bottom right). To approximate the distribution of the sparse supports, we use a dataset of around 4.000 real brain images [6] onto which we apply the 2D DB4 wavelet transform followed by a thresholding operation with a threshold of around 0.006, yielding the weight matrix W (top right). Plugging these weights into formula (9) and normalising the resulting density to 1, we get the adapted subsampling distribution π (top left). We compare this strategy to the above mentioned polynomial decaying density (top middle). We sample 10% of frequencies in the k-space (bottom left and middle). Finally, an application of the NESTA algorithm to solve (1) for both sets of measurements yields the results in the figure. As can be seen, the adapted subsampling strategy is able to outperform the quadratically decaying subsampling strategy.

To show that our new subsampling strategy does indeed adapt to the underlying distribution of sparse supports, we repeat the above experiment but this time use a different dataset — the MRNet dataset which consists of around 30.000 images of knees [16] — to generate the weight matrix W (Figure 3). Again we transform each training image into the DB4 wavelet basis and apply a threshold of about 0.006 to get distribution of non-zero coefficients

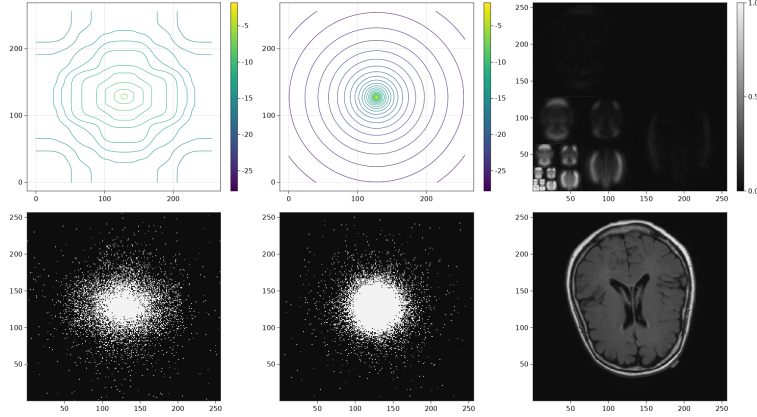


Figure 2: Adapted variable density sampling scheme (left column) vs polynomial decay (middle column). Weight matrix W of sparse support in the DB4 wavelet basis (top right) and test image (bottom right). The resulting PSNR values are: Adapted - 32.8 and Polynomial - 32.0.

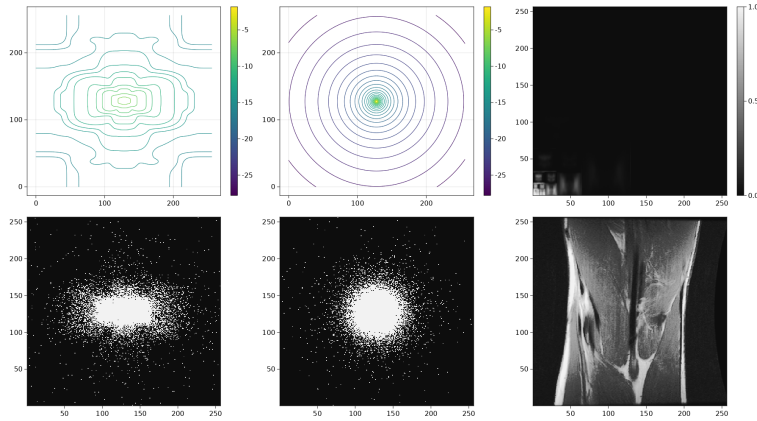


Figure 3: Adapted variable density sampling scheme (left column) vs polynomial decay (middle column). Weight matrix W of sparse distribution in the DB4 wavelet basis (top right) and test image (bottom right). The resulting PSNR values are: Adapted - 27.9 and Polynomial - 26.8.

(top right). This time the resulting weights are non-symmetrical and hence plugging them into formula (9) results in a non-symmetrical subsampling density, thereby *adapting* to the underlying structure of the signals. Sampling 10% of measurements from the adapted and polynomial densities (bottom left and middle), we get by applying the NESTA algorithm to (1) that our adapted subsampling scheme outperforms the heuristically inspired polynomial subsampling strategy.

This difference in performance gets even more pronounced in the next experiment (Figure 4),

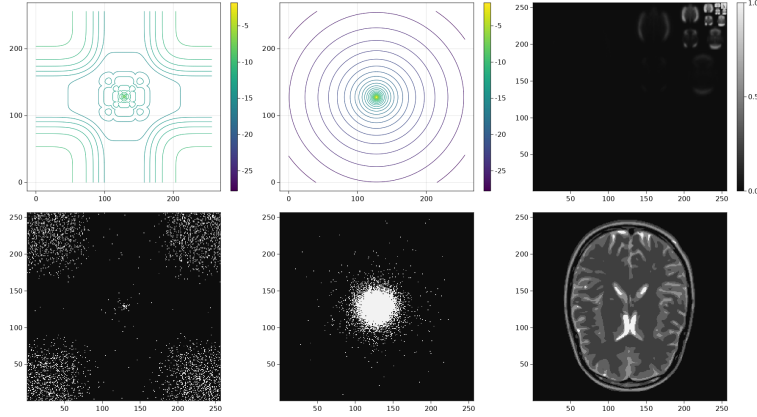


Figure 4: Adapted variable density sampling scheme (left column) vs polynomial decay (middle column). Weight matrix W of sparse distribution in the DB4 wavelet basis (top right) and test image (bottom right). The resulting PSNR values are: Adapted - 22.9 and Polynomial - 11.6.

where we use the same setup (and dataset) as in the first experiment, but **flip** the sparse coefficients of each image (including the test image) by applying the transform $x \mapsto x^f \in \mathbb{C}^K$, $x_1^f = x_K, x_2^f = x_{K-1}, \dots, x_K^f = x_1$ to the vectorised sparse coefficients. This is inspired by the so-called flip test [2]. Obviously, the estimated distribution of the sparse supports is now flipped as well and plugging these weights ω into formula (9) yields a completely different sampling distribution. We again sample 10% of measurements from the 2D k-space (bottom left and middle). This time, our adapted subsampling strategy easily outperforms the heuristic polynomial decay subsampling strategy — resulting in a PSNR value of 22.7 compared to 12.0. As expected, our adapted subsampling strategy is able to use the knowledge of the distribution to derive a subsampling strategy adapted to the signals at hand.

6.1 Blocks of measurements Fourier - DB4

Probably the most interesting application of them all is by using blocks of measurements—Figure 5. We conduct two experiments, first by measuring along horizontal lines in the 2D k-space (left column) and then by measuring square blocks of size 16×16 in the 2D k-space (middle column). We again use the Brain dataset with a threshold of around 0.023 to generate a estimate of the weight matrix W in the separable 2D DB4 wavelet basis (top right). Plugging these estimated weights into formula (7) we get an adapted sampling distribution on the vertical lines (top left) and on the square blocks (top middle). Sampling 20% of measurements from the 2D k-space (middle row) we get good reconstruction of the reference image (bottom right) for both measurement techniques (bottom left and middle). This shows how our results also apply to the setting of blocks of measurements.

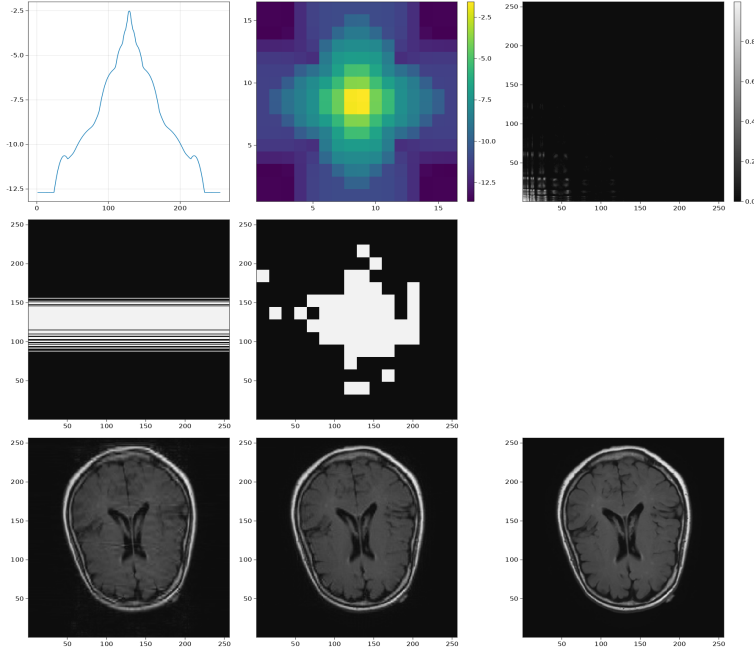


Figure 5: Adapted variable density sampling schemes with vertical lines (left column) and squares (middle column). Weight matrix W of sparse distribution in the separable 2D DB4 wavelet basis (top right), test image (bottom right) and reconstructions (bottom left and middle). The resulting PSNR values are: Lines - 29.9 and Squares - 33.9.

7. Proof of Theorem 3

Note that we have three sources of randomness: the signs σ , the set of random measurements J and the random supports I . Strictly speaking, we are working on the product measure of the three, but in slight abuse of notation, we will write \mathbb{P}_σ , \mathbb{P}_J and \mathbb{P}_I to indicate the probability measure that we use for the corresponding concentration inequalities. The exact statement of Theorem 3 reads as

Theorem 5 *Assume that the signals follow the model in 2, where the support $I \subseteq \mathbb{K}$ is chosen according to the rejective sampling model with probabilities $\omega_1, \dots, \omega_K$ such that $\sum_{k=1}^K \omega_k = S$ and $0 < \omega_k \leq 1$. If the measurements B_k are sampled according to probabilities π_k and if*

$$\begin{aligned} m &\gtrsim \max_k \frac{\|B_k^\star B_k\|_{\infty,1}}{\pi_k} 128 \log(216 \cdot 6K^2/\varepsilon) \log(168K/\varepsilon)^2, \\ m &\gtrsim \max_k \frac{\|B_k D_\omega B_k^\star\|_{2,2}}{\pi_k} \log^2(168K/\varepsilon), \end{aligned} \quad (31)$$

then (1) recovers the sparse signal with probability $1 - \varepsilon$.

Before beginning with the proof, we state 5 concentration inequalities. Recall the definition of the matrices $R_I = \mathbb{I}_I \in \mathbb{R}^{K \times S}$, where $I \subseteq \{1, \dots, K\}$ with $|I| = S$. Define the quantities

$$\Lambda_I := \max_k \frac{\|R_I^* B_k^* B_k R_I\|_{2,2}}{\pi_k m} \quad \text{and} \quad \mu := \max_k \frac{\|B_k^* B_k\|_{\infty,1}}{\pi_k m}.$$

For a fixed support I , the Matrix Bernstein inequality [25] applied to the random matrices $A_I^* A_I - \mathbb{I}$ yields

Lemma 6 (Lemma 2.1 [7], Lemma C.1 [5]) *Let I be a fixed support of cardinality S and let A depend on the draw of the j_ℓ . Then for all $t \geq 0$, we have*

$$\mathbb{P}_J (\|A_I^* A_I - \mathbb{I}\| \geq t) \leq 2S \exp \left(-\frac{t^2/2}{\Lambda_I(1+t)/3} \right).$$

Proof First note that we can write $A_I^* A_I - \mathbb{I}$ as

$$R_I^* A^* A R_I - \mathbb{I} = \sum_{k=1}^m \frac{R_I^* B_{j_k}^* B_{j_k} R_I}{\pi_{j_k} m} - \mathbb{I} = \sum_{k=1}^m \frac{1}{m} \left(\frac{R_I^* B_{j_k}^* B_{j_k} R_I}{\pi_{j_k}} - \mathbb{I} \right) = \sum_{k=1}^m X_k,$$

where $X_k := \frac{1}{m} \left(\frac{R_I^* B_{j_k}^* B_{j_k} R_I}{\pi_{j_k}} - \mathbb{I} \right)$. By definition of the j_k , we have $\mathbb{E}[X_k] = 0$. Further

$$\|X_k\|_{2,2} \leq \frac{1}{m} \max \left(\max_k \frac{\|R_I^* B_k^* B_k R_I\|_{2,2}}{\pi_k} - 1, 1 \right) \leq \Lambda_I.$$

To bound the variance, we note

$$\begin{aligned} 0 \preceq \mathbb{E}[X_k^2] &= \mathbb{E} \left[\left(\frac{R_I^* B_{j_k}^* B_{j_k} R_I}{\pi_{j_k} m} \right)^2 \right] - \frac{1}{m^2} \mathbb{I} \\ &\preceq \Lambda_I \mathbb{E} \left[\frac{R_I^* B_{j_k}^* B_{j_k} R_I}{\pi_{j_k} m} \right] \preceq \Lambda_I \frac{1}{m} \mathbb{I}, \end{aligned}$$

which leads to $\sigma^2 = \|\sum_{k=1}^m \mathbb{E}[X_k^2]\|_{2,2} \leq \Lambda_I$. An application of the Matrix Bernstein inequality yields the result. \blacksquare

Further, for I fixed, and $i \in I^c$, we are going to apply the vector Bernstein inequality [19] on $\|A_I^* A_i\|_2$. Together with a union bound this yields

Lemma 7 *Let I be a fixed support of cardinality S and let A depend on the draw of the j_ℓ . Then for all $t \geq \frac{1}{6}(\sqrt{\mu \Lambda_I} + \sqrt{\mu \Lambda_I + 36 \Lambda_I})$, we have*

$$\mathbb{P}_J \left(\max_{i \in I^c} \|A_I^* A_i\|_2 \geq t \right) \leq 28K \exp \left(-\frac{t^2/2}{\Lambda_I + \sqrt{\Lambda_I \mu t}/3} \right).$$

Proof Fix $i \in I^c$. Then

$$\|A_I^* A_i\|_2 = \left\| \sum_{k=1}^m \frac{1}{m} \frac{R_I^* B_{j_k}^* B_{j_k} e_i}{\pi_{j_k}} \right\|_2 = \left\| \sum_{k=1}^m X_k \right\|_2.$$

Since $i \in I^c$, we have $\mathbb{E}[X_k] = \frac{1}{m} R_I^* \sum_{\ell=1}^M B_\ell B_\ell^* e_i = 0$. Further

$$\max_k \|X_k\|_2 = \max_k \left\| \frac{R_I^* B_k^* B_k e_i}{\pi_k m} \right\|_2 \leq \sqrt{\Lambda_I} \sqrt{\mu}$$

To bound the variance, note

$$\begin{aligned} \mathbb{E}[\|X_k\|_2^2] &= \mathbb{E} \left[\left\| \frac{R_I^* B_{j_k}^* B_{j_k} e_i}{\pi_{j_k} m} \right\|_2^2 \right] \leq \\ &\leq \Lambda_I \mathbb{E} \left[\left\| \frac{B_{j_k} e_i}{\sqrt{\pi_{j_k} m}} \right\|_2^2 \right] = \Lambda_I \|e_i\|_2^2 \frac{1}{m} = \Lambda_I \frac{1}{m}. \end{aligned}$$

This leads to $\sigma^2 = \sum_{k=1}^m \mathbb{E}[\|X_k\|_2^2] \leq \Lambda_I$. A union bound finishes the proof. \blacksquare

For convenience we restate an easy consequence of Hoeffding's inequality.

Lemma 8 (Hoeffding [17]) *Let $M \in \mathbb{C}^{K \times S}$ be a matrix and $x \in \mathbb{R}^S$ such that $\text{sign}(x) \in \mathbb{R}^S$ is an independent Rademacher sequence. Then, for all $t \geq 0$*

$$\mathbb{P}_\sigma (\|Mx\|_\infty \geq t) \leq 2K \exp \left(-\frac{t^2}{2\|M\|_{\infty,2}^2 \|x\|_\infty^2} \right).$$

The key ingredient to prove Theorem 3 is the following concentration inequality for the operator norm of random submatrices with non-uniformly distributed supports which can be found in [23]². This is what allows us to go one step further than existing results in analysing the underlying relationship between the sensing matrix and the distribution of sparse supports.

Lemma 9 ([23]) *Let $H \in \mathbb{C}^{K \times K}$ be a matrix with zero diagonal. Assume that the support $I \subseteq \mathbb{K}$ is chosen according to the rejective sampling model with probabilities $\omega_1, \dots, \omega_K$ such that $\sum_{i=1}^K \omega_i = S$. Further let ω denote the corresponding weight vectr. If $t \geq 2e^2 \|D_\omega^{\frac{1}{2}} H D_\omega^{\frac{1}{2}}\|$ and*

$$\begin{aligned} \|H\|_{\infty,1} &\leq \frac{t}{2 \log(216K/\varepsilon)} \\ \|H D_\omega^{\frac{1}{2}}\|_{\infty,2}^2 &\leq \frac{t^2}{4e^2 \log(216K/\varepsilon)}, \end{aligned}$$

then $\mathbb{P}_I(\|R_I^* H R_I\| \geq t) \leq \varepsilon$.

Now we are finally able to state the proof of Theorem 3.

Proof

From [24, 14] we know that if $\|A_{I^c}^* A_I (A_I^* A_I)^{-1} \sigma_I\|_\infty < 1$, then x is the unique solution of the ℓ_1 -minimisation problem (1). Set $M := A_{I^c}^* A_I (A_I^* A_I)^{-1}$ and assume that $\vartheta_I := \|A_I^* A_I - \mathbb{I}\| \leq 1/2$. Then

$$\|M\|_{\infty,2} = \|A_{I^c}^* A_I (A_I^* A_I)^{-1}\|_{\infty,2} \leq \|A_{I^c}^* A_I\|_{\infty,2} \|(A_I^* A_I)^{-1}\|_{2,2} \leq 2\|A_{I^c}^* A_I\|_{\infty,2}.$$

2. The result in the cited paper is stated only for real matrices, but a careful analysis of the proof shows that this result also holds for complex matrices.

Noting that $\|A_{I^c}^* A_I\|_{\infty,2} = \max_{i \in I^c} \|A_I^* A_i\|_2$ we have

$$\begin{aligned} \mathbb{P}(\|M\sigma\|_{\infty} \geq 1) &\leq \mathbb{P}_{\sigma}(\|M\sigma\|_{\infty} \geq 1 \mid \|M\|_{\infty,2} \leq 2\gamma) \\ &\quad + \mathbb{P}(\|A_I^* A_I - \mathbb{I}\| \geq 1/2) + \mathbb{P}\left(\max_{i \in I^c} \|A_I^* A_i\|_2 \geq \gamma\right) \end{aligned}$$

Setting $\gamma^2 = \frac{1}{8 \log(6K/\varepsilon)}$ and applying Lemma 8 to $M\sigma$ yields that the first term on the right hand side is bound by $\varepsilon/3$. Further

$$\begin{aligned} &\mathbb{P}(\|A_I^* A_I - \mathbb{I}\| \geq 1/2) + \mathbb{P}\left(\max_{i \in I^c} \|A_I^* A_i\|_2 \geq \gamma\right) \\ &\leq \mathbb{P}_J\left(\|A_I^* A_I - \mathbb{I}\| \geq 1/2 \mid \Lambda_I \leq v\right) + \mathbb{P}_I(\Lambda_I \geq v) \\ &\quad + \mathbb{P}_J\left(\max_{i \in I^c} \|A_I^* A_i\|_2 \geq \gamma \mid \Lambda_I \leq v\right) + \mathbb{P}_I(\Lambda_I \geq v) \end{aligned}$$

Setting $v := \frac{1}{32 \log^2(168K/\varepsilon)}$ and using that by the assumptions in Theorem 3

$$\mu \leq \frac{1}{128 \log(216 \cdot 6K^2/\varepsilon) \log^2(168K/\varepsilon)},$$

an application Lemma 6 and Lemma 7 yield that

$$\mathbb{P}(\|A_I^* A_I - \mathbb{I}\| \geq 1/2) + \mathbb{P}\left(\max_{i \in I^c} \|A_I^* A_i\|_2 \geq \gamma\right) \leq \varepsilon/3 + 2\mathbb{P}_I(\Lambda_I \geq v).$$

So to finish the proof we have to show that $\mathbb{P}(\Lambda_I \geq v) \leq \varepsilon/6$. To that end define the matrices

$$H_k := \frac{(B_k^* B_k - \text{diag}(B_k^* B_k))}{\pi_k m}.$$

By our assumptions, we have

$$\Lambda_I \leq \max_k \|R_I^* H_k R_I\| + \|\text{diag}\left(\frac{R_I^* B_k^* B_k R_I}{\pi_k m}\right)\| \leq \max_k \|R_I^* H_k R_I\| + \mu \leq \max_k \|H_k\| + v/2.$$

So we have to show that $\mathbb{P}(\max_k \|R_I^* H_k R_I\| \geq v/2) \leq \varepsilon/6$, which we will do by showing that $\mathbb{P}(\|R_I^* H_k R_I\| \geq v/2) \leq \varepsilon/(6K)$ together with a union bound. By applying 9 to each H_k this is satisfied, if

$$\begin{aligned} \|H_k D_{\omega}^{\frac{1}{2}}\|_{\infty,2}^2 &\leq \frac{(v/2)^2}{4e^2 \log(216 \cdot 6K^2/\varepsilon)} \\ \|H_k\|_{\infty,1} &\leq \mu \leq \frac{v/2}{2 \log(216 \cdot 6K^2/\varepsilon)}, \end{aligned}$$

and $v \geq 2e^2 \|D_{\omega}^{\frac{1}{2}} H_k D_{\omega}^{\frac{1}{2}}\|$. Using that $\|H_k D_{\omega}^{\frac{1}{2}}\|_{\infty,2}^2 \leq \mu \max_k \|B_k D_{\omega} B_k^*\|$ this follows from the assumptions in Theorem 3.

Remark 10 *The proof of our main result relies heavily on the random signs of our signals. One could remove this assumption by instead employing the so-called "golfing scheme" proposed in [15]. Following the argument in [7] one should be able to derive similar results in the case of deterministic sign patterns. Since this would not have any impact on the optimal sampling distribution we opted for the shorter proof presented here.*

■

8. Discussion

The above results showed that the optimal variable density subsampling strategy should not only depend on the structure of the sensing and sparsity matrices, but also on the distribution of sparsity patterns of the signals to be measured. We derived lower bounds on the number of measurements to ensure recovery of the sparse signals with high probability and derived a simple formula for the optimal subsampling strategy. We showed that this distribution can be estimated from a training set and that the resulting adapted subsampling scheme provides state of the art performance in a range of situations. For future work it would be interesting to analyse different settings of blocks of measurements, where explicit lower bounds on the number of measurements can be derived.

Acknowledgments

This work was supported by the Austrian Science Fund (FWF) under Grant no. Y760. Finally, many thanks go to Karin Schnass for her availability for discussion and her helpful input.

References

- [1] B. Adcock, A.C. Hansen, and B. Roman. A note on compressed sensing of structured sparse wavelet coefficients from subsampled fourier measurements. *IEEE Signal Processing Letters*, 23(5):732–736, 2016. doi: 10.1109/LSP.2016.2550101.
- [2] B. Adcock, A.C. Hansen, C. Poon, and B. Roman. Breaking the coherence barrier: A new theory for compressed sensing. *Forum of Mathematics, Sigma*, 5, 2017.
- [3] B. Adcock, C. Boyer, and S. Brugiapaglia. On oracle-type local recovery guarantees in compressed sensing. *Information and Inference: A Journal of the IMA*, 10(1):1–49, 2020. doi: 10.1093/imaiai/iaaa007.
- [4] S. Becker, J. Bobin, and E. Candès. Nesta: A fast and accurate first-order method for sparse recovery. *SIAM Journal on Imaging Sciences*, 4(1):1–39, 2011. doi: 10.1137/090756855. URL <https://doi.org/10.1137/090756855>.
- [5] C. Boyer, P. Weiss, and J. Bigot. Compressed sensing with structured sparsity and structured acquisition. *Applied and Computational Harmonic Analysis*, 46(2):312 – 350, 2019.

- [6] M. Buda. Brain MRI segmentation. <https://www.kaggle.com/datasets/mateuszbuda/lgg-mri-segmentation>, 2019. Accessed: 2022-06-27.
- [7] E. Candès and Y. Plan. A probabilistic and riplless theory of compressed sensing. *IEEE Transactions on Information Theory*, 57(11):7235–7254, 2011.
- [8] E. Candès, J. Romberg, and T. Tao. Robust uncertainty principles: exact signal reconstruction from highly incomplete frequency information. *IEEE Transactions on Information Theory*, 52(2):489–509, 2006. doi: 10.1109/TIT.2005.862083.
- [9] N. Chauffert, P. Ciuciu, J. Kahn, and P. Weiss. Variable density sampling with continuous trajectories. *SIAM Journal on Imaging Sciences*, 7, 11 2013.
- [10] N. Chauffert, P. Ciuciu, and P. Weiss. Variable density compressed sensing in MRI. Theoretical vs heuristic sampling strategies. In *2013 IEEE 10th International Symposium on Biomedical Imaging*, pages 298–301, 2013.
- [11] I.Y. Chun and B. Adcock. Compressed sensing and parallel acquisition. *IEEE Transactions on Information Theory*, 63(8):4860–4882, 2017. doi: 10.1109/TIT.2017.2700440.
- [12] D.L. Donoho. Compressed sensing. *IEEE Transactions on Information Theory*, 52(4):1289–1306, 2006. doi: 10.1109/TIT.2006.871582.
- [13] D.L. Donoho, M. Elad, and V.N. Temlyakov. Stable recovery of sparse overcomplete representations in the presence of noise. *IEEE Transactions on Information Theory*, 52(1):6–18, January 2006.
- [14] J. Fuchs. On sparse representations in arbitrary redundant bases. *IEEE Transactions on Information Theory*, 50:1341–1344, 2004.
- [15] D. Gross. Recovering low-rank matrices from few coefficients in any basis. *IEEE Transactions on Information Theory*, 57(3):1548–1566, 2011.
- [16] Stanford ML group. MRNet Dataset. <https://stanfordmlgroup.github.io/competitions/mrnet/>, 2019. Accessed: 2022-06-27.
- [17] W. Hoeffding. Probability inequalities for sums of bounded random variables. *Journal of the American Statistical Association*, 58(301):13–30, 1963. doi: 10.1080/01621459.1963.10500830. URL <https://www.tandfonline.com/doi/abs/10.1080/01621459.1963.10500830>.
- [18] F. Krahmer and R. Ward. Stable and robust sampling strategies for compressive imaging. *IEEE Transactions on Image Processing*, 23(2):612–622, 2014.
- [19] S. Minsker. On some extensions of bernstein’s inequality for self-adjoint operators. *Statistics and Probability Letters*, 127:111–119, 2017. ISSN 0167-7152.
- [20] Y. Nesterov. Smooth minimization of nonsmooth functions. *Math. Programming*, pages 127–152, 2005.

- [21] G. Puy, P. Vandergheynst, and Y. Wiaux. On variable density compressive sampling. *IEEE Signal Processing Letters*, 18(10):595–598, 2011.
- [22] H. Rauhut. Compressive sensing and structured random matrices. In M. Fornasier, editor, *Theoretical Foundations and Numerical Methods for Sparse Recovery*, Radon Series on Computational and Applied Mathematics. De Gruyter Verlag, 2010.
- [23] S. Ruetz and K. Schnass. Submatrices with non-uniformly selected random supports and insights into sparse approximation. *SIAM Journal on Matrix Analysis and Applications*, 42(3):1268–1289, 2021.
- [24] J. Tropp. Recovery of short, complex linear combinations via l1 minimization. *IEEE Transactions on Information Theory*, 51:1568–1570, 2005.
- [25] J. Tropp. User-friendly tail bounds for sums of random matrices. *Foundations of Computational Mathematics*, 12(4):389–434, 2012.